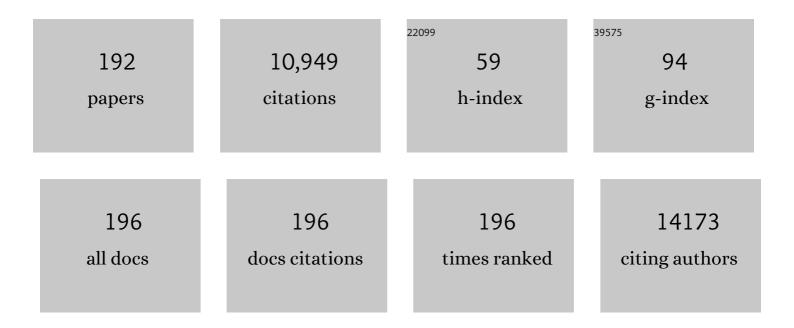
Yan Shen

List of Publications by Year in descending order

Source: https://exaly.com/author-pdf/6245633/publications.pdf Version: 2024-02-01



VAN SHEN

#	Article	IF	CITATIONS
1	Hole Selective NiO Contact for Efficient Perovskite Solar Cells with Carbon Electrode. Nano Letters, 2015, 15, 2402-2408.	4.5	412
2	Scanning Electrochemical Microscopy for Direct Imaging of Reaction Rates. Angewandte Chemie - International Edition, 2007, 46, 1584-1617.	7.2	361
3	Engineering NiS/Ni ₂ P Heterostructures for Efficient Electrocatalytic Water Splitting. ACS Applied Materials & Interfaces, 2018, 10, 4689-4696.	4.0	312
4	Aminoâ€Functionalized Conjugated Polymer as an Efficient Electron Transport Layer for Highâ€Performance Planarâ€Heterojunction Perovskite Solar Cells. Advanced Energy Materials, 2016, 6, 1501534.	10.2	278
5	Efficient screen printed perovskite solar cells based on mesoscopic TiO2/Al2O3/NiO/carbon architecture. Nano Energy, 2015, 17, 171-179.	8.2	261
6	Carbon Quantum Dots/TiO _{<i>x</i>} Electron Transport Layer Boosts Efficiency of Planar Heterojunction Perovskite Solar Cells to 19%. Nano Letters, 2017, 17, 2328-2335.	4.5	211
7	A Power Pack Based on Organometallic Perovskite Solar Cell and Supercapacitor. ACS Nano, 2015, 9, 1782-1787.	7.3	201
8	Efficient Planar Perovskite Solar Cells with Improved Fill Factor via Interface Engineering with Graphene. Nano Letters, 2018, 18, 2442-2449.	4.5	195
9	Flexible Supercapacitors Based on Bacterial Cellulose Paper Electrodes. Advanced Energy Materials, 2014, 4, 1301655.	10.2	182
10	Electronic modulation of transition metal phosphide <i>via</i> doping as efficient and pH-universal electrocatalysts for hydrogen evolution reaction. Chemical Science, 2018, 9, 1970-1975.	3.7	176
11	Freestanding bacterial cellulose–polypyrrole nanofibres paper electrodes for advanced energy storage devices. Nano Energy, 2014, 9, 309-317.	8.2	167
12	Subtle Balance Between Length Scale of Phase Separation and Domain Purification in Smallâ€Molecule Bulkâ€Heterojunction Blends under Solvent Vapor Treatment. Advanced Materials, 2015, 27, 6296-6302.	11.1	159
13	Electrochemical Design of Ultrathin Platinum-Coated Gold Nanoparticle Monolayer Films as a Novel Nanostructured Electrocatalyst for Oxygen Reduction. Journal of Physical Chemistry B, 2004, 108, 8142-8147.	1.2	158
14	Electrochemistry and Electrogenerated Chemiluminescence of SiO2Nanoparticles/Tris(2,2â€~-bipyridyl)ruthenium(ΙΙ) Multilayer Films on Indium Tin Oxide Electrodes. Analytical Chemistry, 2004, 76, 184-191.	3.2	155
15	14.7% efficient mesoscopic perovskite solar cells using single walled carbon nanotubes/carbon composite counter electrodes. Nanoscale, 2016, 8, 6379-6385.	2.8	151
16	Highly Efficient Perovskite Solar Cells with Gradient Bilayer Electron Transport Materials. Nano Letters, 2018, 18, 3969-3977.	4.5	147
17	Photovoltaic behaviour of lead methylammonium triiodide perovskite solar cells down to 80 K. Journal of Materials Chemistry A, 2015, 3, 11762-11767.	5.2	135
18	Will organic–inorganic hybrid halide lead perovskites be eliminated from optoelectronic applications?. Nanoscale Advances, 2019, 1, 1276-1289.	2.2	130

#	Article	IF	CITATIONS
19	Artificial photosynthesis of ethanol using type-II g-C3N4/ZnTe heterojunction in photoelectrochemical CO2 reduction system. Nano Energy, 2019, 60, 827-835.	8.2	126
20	Detection of Hydrogen Peroxide Produced during Electrochemical Oxygen Reduction Using Scanning Electrochemical Microscopy. Analytical Chemistry, 2008, 80, 750-759.	3.2	119
21	17% efficient printable mesoscopic PIN metal oxide framework perovskite solar cells using cesium-containing triple cation perovskite. Journal of Materials Chemistry A, 2017, 5, 22952-22958.	5.2	119
22	Enhancing Efficiency of Perovskite Solar Cells via Surface Passivation with Graphene Oxide Interlayer. ACS Applied Materials & Interfaces, 2017, 9, 38967-38976.	4.0	118
23	A perovskite solar cell-TiO ₂ @BiVO ₄ photoelectrochemical system for direct solar water splitting. Journal of Materials Chemistry A, 2015, 3, 21630-21636.	5.2	109
24	New generation perovskite solar cells with solution-processed amino-substituted perylene diimide derivative as electron-transport layer. Journal of Materials Chemistry A, 2016, 4, 8724-8733.	5.2	109
25	Fabrication of a Metalloporphyrinâ^'Polyoxometalate Hybrid Film by a Layer-by-Layer Method and Its Catalysis for Hydrogen Evolution and Dioxygen Reduction. Journal of Physical Chemistry B, 2003, 107, 9744-9748.	1.2	103
26	A New Method for Fitting Current–Voltage Curves of Planar Heterojunction Perovskite Solar Cells. Nano-Micro Letters, 2018, 10, 5.	14.4	102
27	Efficient planar perovskite solar cells using halide Sr-substituted Pb perovskite. Nano Energy, 2017, 36, 213-222.	8.2	100
28	Highly Efficient Perovskite Solar Cells via Nickel Passivation. Advanced Functional Materials, 2018, 28, 1804286.	7.8	100
29	Simultaneous electrochemical determination of ascorbic acid, dopamine and uric acid with helical carbon nanotubes. Electrochimica Acta, 2013, 91, 261-266.	2.6	97
30	Spiro-thiophene derivatives as hole-transport materials for perovskite solar cells. Journal of Materials Chemistry A, 2015, 3, 12139-12144.	5.2	96
31	Black phosphorus quantum dots in inorganic perovskite thin films for efficient photovoltaic application. Science Advances, 2020, 6, eaay5661.	4.7	95
32	Promises and challenges of alloy-type and conversion-type anode materials for sodium–ion batteries. Materials Today Energy, 2019, 11, 46-60.	2.5	90
33	Graphene oxide wrapped CH3NH3PbBr3 perovskite quantum dots hybrid for photoelectrochemical CO2 reduction in organic solvents. Applied Surface Science, 2019, 465, 607-613.	3.1	89
34	Surface Plasmon Resonance Effect in Inverted Perovskite Solar Cells. Advanced Science, 2016, 3, 1500312.	5.6	88
35	Recent progress in efficient hybrid lead halide perovskite solar cells. Science and Technology of Advanced Materials, 2015, 16, 036004.	2.8	87
36	In Situ Growth of Ru Nanoparticles on (Fe,Ni)(OH) ₂ to Boost Hydrogen Evolution Activity at High Current Density in Alkaline Media. Small Methods, 2020, 4, 1900796.	4.6	82

#	Article	IF	CITATIONS
37	Nanocomposite Multilayer Film of Preyssler-Type Polyoxometalates with Fine Tunable Electrocatalytic Activities. Journal of Physical Chemistry B, 2004, 108, 9780-9786.	1.2	81
38	Electrocatalytic Reduction of Oxygen at Multi-Walled Carbon Nanotubes and Cobalt Porphyrin Modified Glassy Carbon Electrode. Electroanalysis, 2004, 16, 1444-1450.	1.5	76
39	Efficient CsSnl ₃ -based inorganic perovskite solar cells based on a mesoscopic metal oxide framework <i>via</i> incorporating a donor element. Journal of Materials Chemistry A, 2020, 8, 4118-4124.	5.2	75
40	Direct electrochemistry of microperoxidase 11 using carbon nanotube modified electrodes. Journal of Electroanalytical Chemistry, 2005, 578, 121-127.	1.9	74
41	Fabrication of Cobalt Porphyrin. Electrochemically Reduced Graphene Oxide Hybrid Films for Electrocatalytic Hydrogen Evolution in Aqueous Solution. Langmuir, 2014, 30, 6990-6998.	1.6	73
42	Self-standing Bi ₂ O ₃ nanoparticles/carbon nanofiber hybrid films as a binder-free anode for flexible sodium-ion batteries. Materials Chemistry Frontiers, 2017, 1, 1615-1621.	3.2	73
43	Active catalysts based on cobalt oxide@cobalt/N-C nanocomposites for oxygen reduction reaction in alkaline solutions. Nano Research, 2014, 7, 1054-1064.	5.8	72
44	Porous Li ₄ Ti ₅ O ₁₂ –TiO ₂ nanosheet arrays for high-performance lithium-ion batteries. Journal of Materials Chemistry A, 2015, 3, 10107-10113.	5.2	72
45	Significant enhancement of the photoelectrochemical activity of WO3 nanoflakes by carbon quantum dots decoration. Carbon, 2016, 105, 387-393.	5.4	72
46	Hybridizing NiCo ₂ O ₄ and Amorphous Ni _{<i>x</i>} Co _{<i>y</i>} Layered Double Hydroxides with Remarkably Improved Activity toward Efficient Overall Water Splitting. ACS Sustainable Chemistry and Engineering, 2019, 7, 4784-4791.	3.2	70
47	Recent progress on stability issues of organic–inorganic hybrid lead perovskite-based solar cells. RSC Advances, 2016, 6, 89356-89366.	1.7	69
48	MoS 2 nanosheet decorated with trace loads of Pt as highly active electrocatalyst for hydrogen evolution reaction. Electrochimica Acta, 2016, 219, 187-193.	2.6	69
49	Preparation of hybrid thin film modified carbon nanotubes on glassy carbon electrode and its electrocatalysis for oxygen reduction. Chemical Communications, 2004, , 34-35.	2.2	68
50	A new strategy of preparing uniform graphitic carbon nitride films for photoelectrochemical application. Carbon, 2017, 117, 343-350.	5.4	68
51	Zinc Porphyrins with a Pyridineâ€Ringâ€Anchoring Group for Dyeâ€ S ensitized Solar Cells. Chemistry - an Asian Journal, 2013, 8, 956-962.	1.7	67
52	Efficient mesoscopic perovskite solar cells based on the CH ₃ NH ₃ PbI ₂ Br light absorber. Journal of Materials Chemistry A, 2015, 3, 9116-9122.	5.2	67
53	20% Efficient Perovskite Solar Cells with 2D Electron Transporting Layer. Advanced Functional Materials, 2019, 29, 1805168.	7.8	67
54	Organic Sensitizers with Pyridine Ring Anchoring Group for p-Type Dye-Sensitized Solar Cells. Journal of Physical Chemistry C, 2014, 118, 16433-16440.	1.5	66

#	Article	IF	CITATIONS
55	Carbon coated Cu2O nanowires for photo-electrochemical water splitting with enhanced activity. Applied Surface Science, 2015, 358, 404-411.	3.1	66
56	Layered Ruddlesden–Popper Efficient Perovskite Solar Cells with Controlled Quantum and Dielectric Confinement Introduced via Doping. Advanced Functional Materials, 2019, 29, 1903293.	7.8	66
57	Advances in design engineering and merits of electron transporting layers in perovskite solar cells. Materials Horizons, 2020, 7, 2276-2291.	6.4	66
58	D–π–A structured porphyrins for efficient dye-sensitized solar cells. Journal of Materials Chemistry A, 2013, 1, 10008.	5.2	64
59	Photoelectrochemical Kinetics of Eosin Y-Sensitized Zinc Oxide Films Investigated by Scanning Electrochemical Microscopy. Chemistry - A European Journal, 2006, 12, 5832-5839.	1.7	63
60	Full printable perovskite solar cells based on mesoscopic TiO2/Al2O3/NiO (carbon nanotubes) architecture. Solar Energy, 2017, 144, 158-165.	2.9	63
61	Efficient carbon dots/NiFe-layered double hydroxide/BiVO4 photoanodes for photoelectrochemical water splitting. Applied Surface Science, 2018, 439, 1065-1071.	3.1	62
62	Li4Ti5O12-TiO2 nanowire arrays constructed with stacked nanocrystals for high-rate lithium and sodium ion batteries. Journal of Power Sources, 2017, 344, 223-232.	4.0	61
63	Rutile-TiO ₂ decorated Li ₄ Ti ₅ O ₁₂ nanosheet arrays with 3D interconnected architecture as anodes for high performance hybrid supercapacitors. Journal of Materials Chemistry A, 2015, 3, 23570-23576.	5.2	60
64	Achieving ordered and stable binary metal perovskite via strain engineering. Nano Energy, 2018, 48, 117-127.	8.2	60
65	Graphene oxide modified hole transport layer for CH3NH3PbI3 planar heterojunction solar cells. Solar Energy, 2016, 131, 176-182.	2.9	59
66	A highly selective tin-copper bimetallic electrocatalyst for the electrochemical reduction of aqueous CO2 to formate. Applied Catalysis B: Environmental, 2019, 259, 118040.	10.8	59
67	Surface modification of NiCo2Te4 nanoclusters: a highly efficient electrocatalyst for overall water-splitting in neutral solution. Applied Catalysis B: Environmental, 2019, 254, 424-431.	10.8	59
68	MAPbl _{3â^'x} Br _x mixed halide perovskites for fully printable mesoscopic solar cells with enhanced efficiency and less hysteresis. Nanoscale, 2016, 8, 8839-8846.	2.8	57
69	Amino-functionalized conjugated polymer electron transport layers enhance the UV-photostability of planar heterojunction perovskite solar cells. Chemical Science, 2017, 8, 4587-4594.	3.7	57
70	Low-Temperature Stable α-Phase Inorganic Perovskite Compounds via Crystal Cross-Linking. Journal of Physical Chemistry Letters, 2019, 10, 200-205.	2.1	57
71	Copper hexacyanoferrate multilayer films on glassy carbon electrode modified with 4-aminobenzoic acid in aqueous solution. Talanta, 2006, 68, 741-747.	2.9	55
72	N/Si co-doped oriented single crystalline rutile TiO ₂ nanorods for photoelectrochemical water splitting. Journal of Materials Chemistry A, 2015, 3, 10020-10025.	5.2	55

#	Article	IF	CITATIONS
73	Atomic-Scale Tailoring of Organic Cation of Layered Ruddlesden–Popper Perovskite Compounds. Journal of Physical Chemistry Letters, 2019, 10, 1813-1819.	2.1	55
74	Highly efficient light harvesting ruthenium sensitizers for dye-sensitized solar cells featuring triphenylamine donor antennas. Journal of Materials Chemistry A, 2014, 2, 4945-4953.	5.2	54
75	Effect of temperature on the efficiency of organometallic perovskite solar cells. Journal of Energy Chemistry, 2015, 24, 729-735.	7.1	54
76	Effective Magnetic Field Regulation of the Radical Pair Spin States in Electrocatalytic CO ₂ Reduction. Journal of Physical Chemistry Letters, 2020, 11, 48-53.	2.1	54
77	Lead Methylammonium Triiodide Perovskiteâ€Based Solar Cells: An Interfacial Chargeâ€Transfer Investigation. ChemSusChem, 2014, 7, 3088-3094.	3.6	51
78	Efficient p-type dye-sensitized solar cells based on disulfide/thiolate electrolytes. Nanoscale, 2013, 5, 7963.	2.8	50
79	Dopant-free 3,3′-bithiophene derivatives as hole transport materials for perovskite solar cells. Journal of Materials Chemistry A, 2016, 4, 3661-3666.	5.2	50
80	A catalyst based on copper-cadmium bimetal for electrochemical reduction of CO2 to CO with high faradaic efficiency. Electrochimica Acta, 2018, 271, 544-550.	2.6	49
81	TiO 2 nanotubes modified with electrochemically reduced graphene oxide for photoelectrochemical water splitting. Carbon, 2014, 80, 591-598.	5.4	47
82	TiO 2 -B@VS 2 heterogeneous nanowire arrays as superior anodes for lithium-ion batteries. Journal of Power Sources, 2017, 350, 87-93.	4.0	47
83	Hierarchical TiO ₂ spheres assisted with graphene for a high performance lithium–sulfur battery. Journal of Materials Chemistry A, 2016, 4, 16454-16461.	5.2	45
84	Electrochemical and electrogenerated chemiluminescence of clay nanoparticles/Ru(bpy)32+ multilayer films on ITO electrodes. Analyst, The, 2004, 129, 657.	1.7	44
85	Electrochemically reduced graphene oxide multilayer films as metal-free electrocatalysts for oxygen reduction. Journal of Materials Chemistry A, 2013, 1, 1415-1420.	5.2	43
86	Enhancing photoelectrochemical water oxidation efficiency via self-catalyzed oxygen evolution: A case study on TiO2. Nano Energy, 2018, 44, 411-418.	8.2	43
87	Phosphorus-doped TiO2-B nanowire arrays boosting robust pseudocapacitive properties for lithium storage. Journal of Power Sources, 2018, 396, 327-334.	4.0	43
88	Stabilization of Inorganic CsPb _{0.5} Sn _{0.5} I ₂ Br Perovskite Compounds by Antioxidant Tea Polyphenol. Solar Rrl, 2020, 4, 1900457.	3.1	43
89	ZnO decorated TiO2 nanosheet composites for lithium ion battery. Electrochimica Acta, 2015, 182, 529-536.	2.6	42
90	RGO modified Ni doped FeOOH for enhanced electrochemical and photoelectrochemical water oxidation. Applied Surface Science, 2018, 436, 974-980.	3.1	42

#	Article	IF	CITATIONS
91	Two-dimensional hetero-nanostructured electrocatalyst of Ni/NiFe-layered double oxide for highly efficient hydrogen evolution reaction in alkaline medium. Chemical Engineering Journal, 2021, 426, 131827.	6.6	42
92	Ultra-thin bacterial cellulose/poly(ethylenedioxythiophene) nanofibers paper electrodes for all-solid-state flexible supercapacitors. Electrochimica Acta, 2018, 271, 624-631.	2.6	41
93	Fabrication of Metalloporphyrin-Polyoxometalyte Hybrid Film by Layer-by-Layer Method and Its Catalysis for Dioxygen Reduction. Electroanalysis, 2002, 14, 1557-1563.	1.5	40
94	Preparation of Multilayer Films Containing Pt Nanoparticles on a Glassy Carbon Electrode and Application as an Electrocatalyst for Dioxygen Reduction. Langmuir, 2003, 19, 5397-5401.	1.6	40
95	Nanocomposite films containing Au nanoparticles formed by electrochemical reduction of metal ions in the multilayer films as electrocatalyst for dioxygen reduction. Analytica Chimica Acta, 2005, 535, 15-22.	2.6	40
96	Carbazole oligomers revisited: new additions at the carbazole 1- and 8-positions. RSC Advances, 2012, 2, 10821.	1.7	40
97	Nanostructured Nickel Cobaltite Antispinel as Bifunctional Electrocatalyst for Overall Water Splitting. Journal of Physical Chemistry C, 2017, 121, 25888-25897.	1.5	39
98	Enhanced photoelectrochemical water splitting using a cobalt-sulfide-decorated BiVO4 photoanode. Chinese Journal of Catalysis, 2022, 43, 433-441.	6.9	39
99	Photoelectrochemical kinetics of Eosin Y-sensitized zinc oxide films investigated by scanning electrochemical microscopy under illumination with different LED. Electrochimica Acta, 2009, 55, 458-464.	2.6	38
100	Photoelectrochemical Water Splitting System—A Study of Interfacial Charge Transfer with Scanning Electrochemical Microscopy. ACS Applied Materials & Interfaces, 2016, 8, 1606-1614.	4.0	38
101	Interface engineering for high-efficiency perovskite solar cells. Journal of Applied Physics, 2021, 129, .	1.1	38
102	MoO3 nanobelts for high-performance asymmetric supercapacitor. Journal of Materials Science, 2019, 54, 13685-13693.	1.7	36
103	Pyrene-conjugated porphyrins for efficient mesoscopic solar cells: the role of the spacer. Journal of Materials Chemistry A, 2014, 2, 17495-17501.	5.2	35
104	Over 8% efficient CsSnI ₃ -based mesoporous perovskite solar cells enabled by two-step thermal annealing and surface cationic coordination dual treatment. Journal of Materials Chemistry A, 2022, 10, 3642-3649.	5.2	35
105	Potassiumâ€Doped Zinc Oxide as Photocathode Material in Dyeâ€Sensitized Solar Cells. ChemSusChem, 2013, 6, 622-629.	3.6	34
106	Hybrid of Fe@Fe3O4 core-shell nanoparticle and iron-nitrogen-doped carbon material as an efficient electrocatalyst for oxygen reduction reaction. Electrochimica Acta, 2015, 174, 933-939.	2.6	34
107	BiOl–TiO ₂ Nanocomposites for Photoelectrochemical Water Splitting. Advanced Materials Interfaces, 2016, 3, 1500273.	1.9	34
108	Coreâ€6hell Structured NiCo ₂ O ₄ @FeOOH Nanowire Arrays as Bifunctional Electrocatalysts for Efficient Overall Water Splitting. ChemCatChem, 2018, 10, 4119-4125.	1.8	34

#	Article	IF	CITATIONS
109	Multifunctional organic–inorganic multilayer films of tris(2,2′-bipyridine)ruthenium and decatungstate. Electrochemistry Communications, 2003, 5, 913-918.	2.3	33
110	Electrodeposited noble metal particles in polyelectrolyte multilayer matrix as electrocatalyst for oxygen reduction studied using SECM. Physical Chemistry Chemical Physics, 2008, 10, 3635.	1.3	32
111	Direct formation of 13- ions in organic cation solution for efficient perovskite solar cells. Solar Energy Materials and Solar Cells, 2018, 185, 111-116.	3.0	32
112	High-rate and stable iron phosphide nanorods anode for sodium-ion battery. Electrochimica Acta, 2019, 314, 142-150.	2.6	32
113	Interconnected SnO ₂ Nanocrystals Electron Transport Layer for Highly Efficient Flexible Perovskite Solar Cells. Solar Rrl, 2020, 4, 1900229.	3.1	31
114	The Role of Synthesis Parameters on Crystallization and Grain Size in Hybrid Halide Perovskite Solar Cells. Journal of Physical Chemistry C, 2017, 121, 17053-17061.	1.5	30
115	Three-dimensional TiO2 nanowire@NiMoO4 ultrathin nanosheet core-shell arrays for lithium ion batteries. Applied Surface Science, 2018, 435, 641-648.	3.1	30
116	Graphene oxide-protected three dimensional Se as a binder-free cathode for Li-Se battery. Electrochimica Acta, 2016, 190, 258-263.	2.6	29
117	Hierarchical CuBi ₂ O ₄ microspheres as lithium-ion battery anodes with superior high-temperature electrochemical performance. RSC Advances, 2017, 7, 13250-13256.	1.7	29
118	Fully Inorganic CsSnI ₃ Mesoporous Perovskite Solar Cells with High Efficiency and Stability via Coadditive Engineering. Solar Rrl, 2021, 5, 2100069.	3.1	29
119	Simple preparation method of Pd nanoparticles on an Au electrode and its catalysis for dioxygen reductionElectronic supplementary information (ESI) available: XRD pattern of an evaporated Au electrode and CVs for the reduction of O2 on a bare Au(111) electrode or a Pd-nanoparticle-film-modified electrode. See: http://www.rsc.org/suppdata/nj/b3/b300566f/. New	1.4	27
120	Preparation of a phosphopolyoxomolybdate P2Mo18O626âî doped polypyrrole modified electrode and its catalytic properties. Journal of Electroanalytical Chemistry, 2004, 566, 63-71.	1.9	27
121	Pt Catalyst Supported within TiO2 Mesoporous Films for Oxygen Reduction Reaction. Electrochimica Acta, 2014, 130, 97-103.	2.6	27
122	Phosphor coated NiO-based planar inverted organometallic halide perovskite solar cells with enhanced efficiency and stability. Applied Physics Letters, 2016, 109, .	1.5	27
123	Regulating the electronic configuration of ruthenium nanoparticles via coupling cobalt phosphide for hydrogen evolution in alkaline media. Materials Today Physics, 2020, 12, 100182.	2.9	27
124	Dâ~'π–A Porphyrin Sensitizers with Ï€-Extended Conjugation for Mesoscopic Solar Cells. Journal of Physical Chemistry C, 2014, 118, 14739-14748.	1.5	26
125	Co9S8 hollow spheres for enhanced electrochemical detection of hydrogen peroxide. Talanta, 2015, 141, 73-79.	2.9	26
126	Synthesis, characterization and fabrication on a glassy carbon electrode of a tetra-iron substituted sandwich-type pentadecatungstodiarsenate heteropolyanionElectronic supplementary information (ESI) available: model of layer formation, CV of 4-ABA on a GCE and of QPVP-Os/4-ABA/GCE in pH 4.7 buffer, plots of Ed vs. log (i/id – i) and XRD of the title compound. See http://www.rsc.org/suppdata/nj/b2/b205766m/. New Journal of Chemistry, 2003, 27, 756-764.	1.4	25

#	Article	IF	CITATIONS
127	Disulfide/Thiolate Based Redox Shuttle for Dye-Sensitized Solar Cells: An Impedance Spectroscopy Study. Journal of Physical Chemistry C, 2012, 116, 25233-25241.	1.5	25
128	Stability Issue of Perovskite Solar Cells under Realâ€World Operating Conditions. Energy Technology, 2020, 8, 1900744.	1.8	25
129	Modulated growth of high-quality CsPbI ₃ perovskite film using a molybdenum modified SnO ₂ layer for highly efficient solar cells. Journal of Materials Chemistry A, 2021, 9, 25567-25575.	5.2	25
130	Near Field Enhanced Photocurrent Generation in P-type Dye-Sensitized Solar Cells. Scientific Reports, 2014, 4, 3961.	1.6	24
131	Temperature Dependent Characteristics of Perovskite Solar Cells. ChemistrySelect, 2017, 2, 4469-4477.	0.7	24
132	Novel donor-acceptor-donor structured small molecular hole transporting materials for planar perovskite solar cells. Journal of Energy Chemistry, 2019, 32, 85-92.	7.1	23
133	Electrochemically Deposited CoS Films as Counter Electrodes for Efficient Quantum Dot-Sensitized Solar Cells. Journal of the Electrochemical Society, 2013, 160, H624-H629.	1.3	22
134	Hierarchical WO 3 nanoflakes architecture with enhanced photoelectrochemical activity. Electrochimica Acta, 2017, 225, 473-481.	2.6	22
135	Cation-Assisted Restraint of a Wide Quantum Well and Interfacial Charge Accumulation in Two-Dimensional Perovskites. ACS Energy Letters, 2018, 3, 1815-1823.	8.8	22
136	Hydrogen peroxide biosensor based on microperoxidase-11 immobilized on flexible MWCNTs-BC nanocomposite film. Talanta, 2015, 131, 243-248.	2.9	21
137	AgBi3I10 rudorffite for photovoltaic application. Solar Energy, 2020, 206, 436-442.	2.9	21
138	Electrochemical behavior and assembly of tetranuclear Dawson-derived sandwich compound [Cd4(H2O)2(As2W15O56)2]16â^' on 4-aminobenzoic acid modified glassy carbon electrode. Analytica Chimica Acta, 2005, 534, 343-351.	2.6	20
139	Investigation of Regeneration Kinetics in Quantum-Dots-Sensitized Solar Cells with Scanning Electrochemical Microscopy. ACS Applied Materials & amp; Interfaces, 2014, 6, 20913-20918.	4.0	20
140	Investigation of Dye Regeneration Kinetics in Sensitized Solar Cells by Scanning Electrochemical Microscopy. ChemPhysChem, 2014, 15, 1182-1189.	1.0	20
141	Investigation on regeneration kinetics at perovskite/oxide interface with scanning electrochemical microscopy. Journal of Materials Chemistry A, 2015, 3, 9216-9222.	5.2	19
142	Large active layer thickness toleration of high-efficiency small molecule solar cells. Journal of Materials Chemistry A, 2015, 3, 22274-22279.	5.2	19
143	Bouquetâ€Like NiCo ₂ O ₄ @CoNi ₂ S ₄ Arrays for Highâ€Performance Pseudocapacitors. ChemElectroChem, 2017, 4, 607-612.	1.7	17
144	Interfacial engineering of bismuth with reduced graphene oxide hybrid for improving CO2 electroreduction performance. Electrochimica Acta, 2020, 357, 136840.	2.6	17

#	Article	IF	CITATIONS
145	Effect of a Cocatalyst on a Photoanode in Water Splitting: A Study of Scanning Electrochemical Microscopy. Analytical Chemistry, 2021, 93, 12221-12229.	3.2	17
146	Mn ₃ O ₄ /Carbon Nanotube Nanocomposites as Electrocatalysts for the Oxygen Reduction Reaction in Alkaline Solution. ChemElectroChem, 2014, 1, 1531-1536.	1.7	16
147	Ultrafast synthesis of Te nanorods as cathode materials for lithium-tellurium batteries. Journal of Power Sources, 2017, 371, 48-54.	4.0	16
148	Sea coral-like NiCo ₂ O ₄ @(Ni, Co)OOH heterojunctions for enhancing overall water-splitting. Catalysis Science and Technology, 2018, 8, 4151-4158.	2.1	16
149	Recent progress in inorganic tin perovskite solar cells. Materials Today Energy, 2022, 23, 100891.	2.5	16
150	A cyclopenta[1,2-b:5,4-b′]dithiophene–porphyrin conjugate for mesoscopic solar cells: a D–π–D–A approach. Physical Chemistry Chemical Physics, 2014, 16, 24755-24762.	1.3	15
151	Preparation of hybrid films containing gold nanoparticles and cobalt porphyrin with flexible electrochemical properties. Thin Solid Films, 2013, 545, 327-331.	0.8	14
152	Visualized acid–base discoloration and optoelectronic investigations of azines and azomethines having double 4-[N,N-di(4-methoxyphenyl)amino]phenyl terminals. Journal of Materials Chemistry C, 2015, 3, 7748-7755.	2.7	14
153	F4TCNQ-doped DEPT-SC as hole transporting material for stable perovskite solar cells. Organic Electronics, 2016, 35, 171-175.	1.4	14
154	Phosphate modified N/Si co-doped rutile TiO 2 nanorods for photoelectrochemical water oxidation. Applied Surface Science, 2017, 391, 288-294.	3.1	14
155	Efficient Activation and Electroreduction of Carbon Dioxide on an Electrocatalyst Cadmium Carbonate. ACS Applied Energy Materials, 2021, 4, 2073-2080.	2.5	14
156	Alkyl-thiophene Functionalized D-Ï€-A Porphyrins for Mesoscopic Solar Cells. Electrochimica Acta, 2015, 179, 187-196.	2.6	13
157	Diketopyrrolopyrrole based D-Ï€-A-Ï€-D type small organic molecules as hole transporting materials for perovskite solar cells. Journal of Energy Chemistry, 2018, 27, 1175-1182.	7.1	13
158	Large Magneto-Current Effect in the Electrochemical Detection of Oxalate in Aqueous Solution. Journal of Physical Chemistry C, 2018, 122, 19880-19885.	1.5	13
159	Nanostructured Ni ₂ SeS on Porous-Carbon Skeletons as Highly Efficient Electrocatalyst for Hydrogen Evolution in Acidic Medium. Inorganic Chemistry, 2020, 59, 6018-6025.	1.9	13
160	Minimizing energy loss in two-dimensional tin halide perovskite solar cells—A perspective. APL Materials, 2021, 9, .	2.2	13
161	Preventing inhomogeneous elemental distribution and phase segregation in mixed Pb-Sn inorganic perovskites via incorporating PbS quantum dots. Journal of Energy Chemistry, 2022, 65, 179-185.	7.1	13
162	Controlling Quantum-Well Width Distribution and Crystal Orientation in Two-Dimensional Tin Halide Perovskites via a Strong Interlayer Electrostatic Interaction. ACS Applied Materials & Interfaces, 2021, 13, 49907-49915.	4.0	13

#	Article	IF	CITATIONS
163	Effect of Hole Transport Layer in Planar Inverted Perovskite Solar Cells. Chemistry Letters, 2016, 45, 89-91.	0.7	12
164	Generating Huge Magnetocurrent by Using Spin-Dependent Dehydrogenation Based on Electrochemical System. Journal of Physical Chemistry C, 2017, 121, 28420-28424.	1.5	12
165	Highly Efficient Hydrogen Production Using a Reformed Electrolysis System Driven by a Single Perovskite Solar Cell. ChemSusChem, 2019, 12, 434-440.	3.6	12
166	2D Materials as Electron Transport Layer for Lowâ€Temperature Solutionâ€Processed Perovskite Solar Cells. Solar Rrl, 2021, 5, 2000566.	3.1	12
167	Investigation of the regeneration kinetics of organic dyes with pyridine ring anchoring groups by scanning electrochemical microscopy. RSC Advances, 2014, 4, 51374-51380.	1.7	11
168	Investigation on In–TiO2 composites as highly efficient elecctrocatalyst for CO2 reduction. Electrochimica Acta, 2020, 340, 135948.	2.6	11
169	Stable and efficient full-printable solar cells using inorganic metal oxide framework and inorganic perovskites. Applied Materials Today, 2020, 20, 100644.	2.3	10
170	Boosting electrocatalytic activity of Ni2P nanosheets via incorporation of Ru nanoparticles for efficient hydrogen generation in alkaline media. Applied Surface Science, 2021, 554, 149560.	3.1	10
171	INVESTIGATION OF DYE-REGENERATION KINETICS AT DYE-SENSITIZED p-TYPE CuCrO2 FILM/ELECTROLYTES INTERFACE WITH SCANNING ELECTROCHEMICAL MICROSCOPY. Nano, 2014, 09, 1440008.	0.5	9
172	Graphene supported platinum nanoparticles as catalyst for oxygen reduction reaction. Chemical Research in Chinese Universities, 2015, 31, 1007-1011.	1.3	9
173	Ultrafine Pt nanoparticle decoration with CoP as highly active electrocatalyst for alcohol oxidation. RSC Advances, 2016, 6, 100437-100442.	1.7	9
174	BiOI/WO3 photoanode with enhanced photoelectrochemical water splitting activity. Frontiers of Optoelectronics, 2018, 11, 367-374.	1.9	9
175	Controlling layered Ruddlesden–Popper perovskites <i>via</i> solvent additives. Nanoscale, 2020, 12, 7330-7338.	2.8	9
176	Efficient and Stable Large-Area Perovskite Solar Cells with Inorganic Perovskite/Carbon Quantum Dot-Graded Heterojunction. Research, 2021, 2021, 9845067.	2.8	9
177	Effect of the molecular weight of poly(3-hexylthiophene) on the performance of solid-state dye-sensitized solar cells. RSC Advances, 2013, 3, 14037.	1.7	8
178	Efficient dye-sensitized solar cells using mesoporous submicrometer TiO ₂ beads. RSC Advances, 2015, 5, 62630-62637.	1.7	8
179	Changing the Sign of Exchange Interaction in Radical Pairs to Tune Magnetic Field Effect on Electrogenerated Chemiluminescence. Journal of Physical Chemistry C, 2015, 119, 8089-8094.	1.5	8
180	A stable self-powered ultraviolet photodetector using CH ₃ NH ₃ PbCl ₃ with weak-light detection capacity under working conditions. Journal of Materials Chemistry C, 2022, 10, 7147-7153.	2.7	8

#	Article	IF	CITATIONS
181	Spin-dependent deprotonation induced giant magnetocurrent in electrochemical cells. Physical Chemistry Chemical Physics, 2016, 18, 9897-9901.	1.3	6
182	Hierarchical MnO ₂ Located on Carbon Nanotubes for Enhanced Electrochemical Performance. ChemElectroChem, 2018, 5, 1525-1531.	1.7	6
183	Constructing two-dimensional heterojunction through decorating covalent organic framework with MoS2 for enhanced photoelectrochemical water oxidation. Journal of Environmental Chemical Engineering, 2022, 10, 106900.	3.3	6
184	Preparation of Pt Nanoparticles Assembled in Multilayer Films. Chemistry Letters, 2002, 31, 550-551.	0.7	5
185	ITO surface modification for inverted organic photovoltaics. Frontiers of Optoelectronics, 2015, 8, 269-273.	1.9	5
186	lron incorporation affecting the structure and boosting catalytic activity of Cox-Fey-P for efficient hydrogen evolution. Applied Surface Science, 2019, 478, 103-109.	3.1	4
187	SINGLE-CRYSTAL X-RAY STRUCTURE AND PROPERTIES OF K10[Ni4(H2O)2(AsW9O34)·4H2O. Synthesis and Reactivity in Inorganic, Metal Organic, and Nano Metal Chemistry, 2002, 32, 967-979.	1.8	2

188 Electrodes: Flexible Supercapacitors Based on Bacterial Cellulose Paper Electrodes (Adv. Energy) Tj ETQq0 0 0 rgBT (Overlock 10 Tf 50 4)

189	Abnormal Magnetic Field Effects on Electrogenerated Chemiluminescence. Scientific Reports, 2015, 5, 9105.	1.6	2
190	Self-Assembly Vertical Graphene-Based MoO3 Nanosheets for High Performance Supercapacitors. Nanomaterials, 2022, 12, 2057.	1.9	1
191	Synthesis, Characterization and Fabrication on a Glassy Carbon Electrode of a Tetra-Iron Substituted Sandwich-Type Pentadecatungstodiarsenate Heteropolyanion ChemInform, 2003, 34, no.	0.1	0
192	A special issue on Optoelectronics for Energy. Frontiers of Optoelectronics, 2018, 11, 315-316.	1.9	0